LARGE EDDY SIMULATION OF FLOW OVER A CIRCULAR CYLINDER HAVING MINIMUM LIFT FLUCTUATIONS

Jinsung Kim
School of Mechanical and Aerospace Engineering, Seoul National University,
Seoul 151-744, Korea
kimjs@rankine.snu.ac.kr

Haecheon Choi
School of Mechanical and Aerospace Engineering, Seoul National University,
Seoul 151-744, Korea
choi@socrates.snu.ac.kr

ABSTRACT

In the present study, we perform a large eddy simulation (LES) of flow over a circular cylinder having minimum lift fluctuations at Re=1600. The flow over a circular cylinder at this Reynolds number is featured by elongated separated shear layer and delayed eddy formation. The local minimum of lift fluctuation occurs around the present Reynolds number due to this long distance between the cylinder and the Kármán vortex roll-up position at which the fluctuating energy is concentrated.

INTRODUCTION

Prediction of drag and lift on a circular cylinder has been one of the most essential subjects in fluid mechanics because of its importance in many engineering applications. In view of structural durability and acoustic noise generation, the fluctuations of these forces have more importance than their mean values. Furthermore, in most cases, lift fluctuations are much larger than drag fluctuations and thus many people focus on the first.

It is well known that the fluctuating load on a circular cylinder shows a local minimum at the crossover Reynolds number ($\mathrm{Re} \simeq 10^3$) between the wake transitional regime and the shear-layer transitional regime and at another local minimum at $\mathrm{Re} \simeq 10^5$ between the shear-layer transitional regime and boundary layer transitional regime (Zdravkovich, 1997). Recently, Norberg (2003) showed from extensive experiment that a local minimum of lift fluctuations occurs at $\mathrm{Re} \simeq 1600$ on a circular cylinder, and called this phenomenon as a *lift crisis* in contrast to the well-known *drag crisis*. For drag crisis, there have been a large amount of studies and now it is well known that, at around the inception of the wall boundary layer transitional regime, the separation bubble due to laminar separation and turbulent reattachment delays the main separation point and reduces drag greatly. On the other hand, the lift crisis is not well understood by now.

Norberg (2003) suggested that augmentation of mode-B type secondary vortices and increased three-dimensionality are responsible for the weakening of the Kármán vortex shedding and cause the lift crisis. However, there are many more aspects to be considered to understand the lift crisis at this Reynolds number. Therefore, in the present study, we perform large eddy simulation of turbulent flow behind a circular cylinder at $\mathrm{Re} = 1600$ to investigate the flow characteristics at minimum lift fluctuations. In the following, we first briefly describe the numerical method and show the result from present simulation. Finally, a possible mechanism of the lift crisis is discussed.

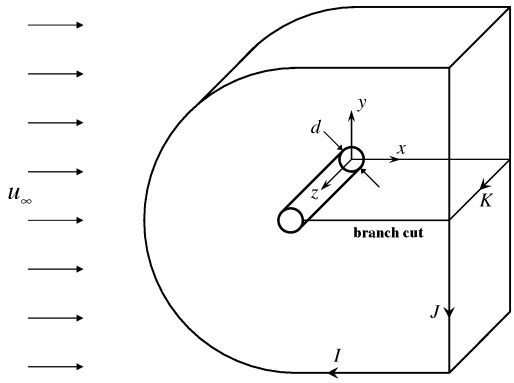

Figure 1: Computational domain and coordinate system.

NUMERICAL METHOD

To investigate the flow over a circular cylinder having a local minimum of lift fluctuations, we carry out large eddy simulation using the dynamic subgrid-scale model (Germano *et al.*, 1991; Lilly, 1992) at $\mathrm{Re} = 1600$. The time integration method is based on a fully implicit, fractional step method. All terms including cross-derivative diffusion terms are advanced with the Crank-Nicolson method in time and are resolved with the second-order central-difference scheme in space. A multigrid method and a Newton iterative method are used to solve the Poisson equation and the discretized nonlinear momentum equations, respectively. See Choi et al. (1993) for the detail.

The computational domain and coordinate system are shown in figure 1. A C-type grid system is used for better resolution in the wake region. Nonuniform grids along the I and J directions ($x - y$ plane) are generated using a hyper-

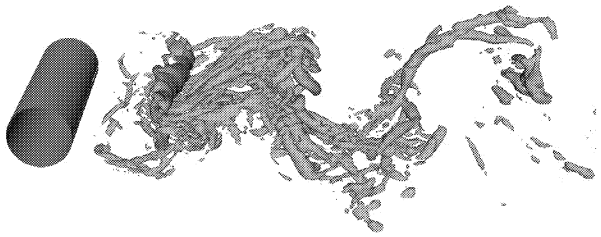

Figure 2: Instantaneous vortical structures.

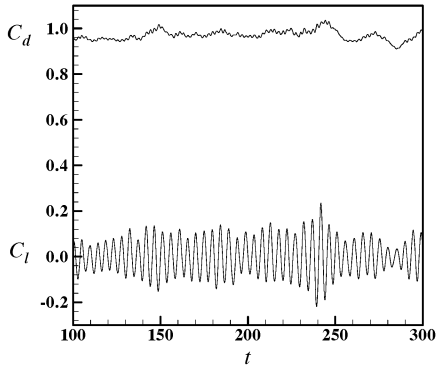

Figure 3: Time histories of the drag and lift coefficients.

bolic grid generation technique, and uniform grids are used in the spanwise direction (z). The size of the computational domain is $-19 \leq x/d \leq 17$, $-25 \leq y/d \leq 25$ and $0 \leq z/d \leq \pi$, where $(x = 0, y = 0)$ corresponds to the center of the cylinder. Numbers of grid points are $672 \times 160 \times 64$. We apply the no-slip condition at the cylinder surface and a Dirichlet boundary condition $(u = u_\infty, v = 0, w = 0)$ is used at the inlet and far field. A periodic boundary condition is used in the spanwise direction and a convective outflow boundary condition, $(\partial u_i/\partial t) + C(\partial u_i/\partial x) = 0$, is used at the exit, where C is the surface-averaged streamwise velocity at the exit.

RESULTS

Figure 2 shows an instantaneous vortical structures. In this figure, the λ_2 vortex identification method of Jeong and Hussain (1995) is used to visualize the vortical structure. We can see large-scale wavy structure in the wake due to the alternating Kármán vortex shedding. Rib-like secondary vortices and smaller scale vortices due to turbulence also can be seen in figure 2. At Re=1600, the boundary layer flow near the cylinder surface and the flow separation are laminar. Thus there is no small-scale vortex around and right behind the cylinder in figure 2.

Time histories of the drag and lift coefficients are shown in figure 3 during about 42 shedding cycles. Periodicity due to the Kármán vortex shedding can be clearly seen. Although the present Reynolds number is close to the lift crisis (that is, the local minimum of the lift fluctuations), the magnitude of lift fluctuation is still much larger than that of drag fluc-

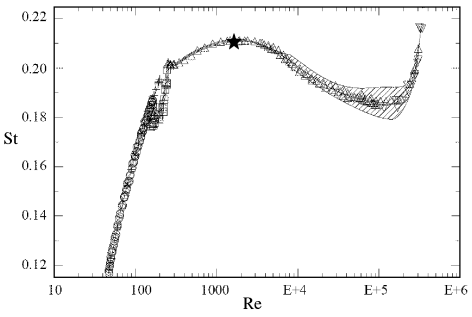

Figure 4: Strouhal number versus Reynolds number. The present result (★) is shown at Re=1600. Other data are from Norberg (2003).

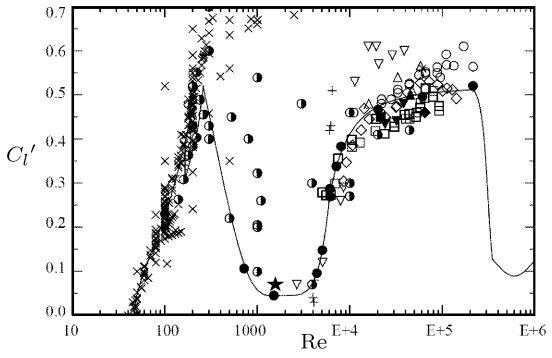

Figure 5: Rms lift fluctuation coefficient versus Reynolds number (from Norberg 2003). The present result (★) is shown at Re=1600.

tuation. The mean value of drag coefficient is $\bar{C}_d = 0.97$ and the rms values of drag and lift coefficients are ${C_d}' = 0.025$ and ${C_l}' = 0.071$, respectively. Note in figure 3 that there exist some variations of C_l in time from one cycle to another and some modulation appears. The Strouhal number calculated from the lift coefficient is St = 0.211 (see figure 4). The present result agrees with the Strouhal number obtained from experiments. Interestingly, the Strouhal number at around the present Reynolds number shows a local maximum in the St-Re relation in figure 4. We will discuss the physical meaning of this high Strouhal number in the next section.

The rms lift fluctuation coefficient from the present LES is shown (★) in figure 5, together with other experimental and numerical results. All other results are compiled by Norberg (2003). Despite the scatter among the results, it is clear that the lift fluctuation shows a local minimum at around Re = 1000 ∼ 3000. The result from present LES agrees well with other results and supports the existence of the lift crisis. It is interesting that the scatter of data is large at the boundaries of the minimum lift zone, i.e., at Re ≈ 1000 and 4000. This implies that the flow at the Reynolds number near the minimum lift fluctuation is very sensitive to the experimental conditions.

Figure 6 shows the rms pressure fluctuations along the cylinder surface, together with experimental ones from Norberg (2003) at Re=720, 1500 and 4400. The present result is in excellent agreement with the experimental data at Re=1500. From his data, we can see an exceptionally low pressure fluc-

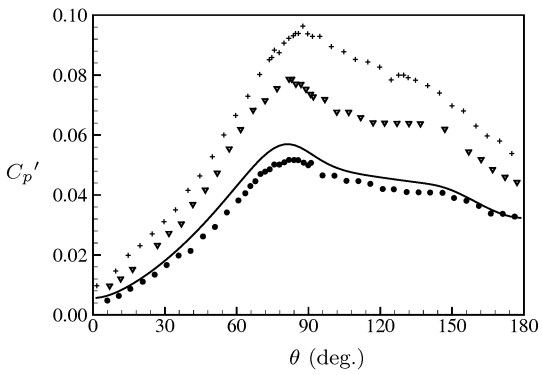

Figure 6: Rms pressure fluctuations along the cylinder surface: ———, present LES (Re = 1600); +, Re=720 (Norberg, 2003); •, Re = 1500 (Norberg, 2003); ▼, Re = 4400 (Norberg, 2003).

tuations at Re=1500.

The time-averaged streamwise velocity and Reynolds shear stress are shown in figures 7a and b, respectively. In figure 7a, the separated shear layers persist down to $x \simeq d$ and then spread out in the downstream. The size of the separation bubble is about $2.2d$, which is in good agreement with experimental measurement (Norberg, 1998). From figure 7b, we can see that the flow near the circular cylinder is almost laminar, and turbulence appears at $x \geq d$. From these observations it is clear that the cylinder is less exposed to vortex shedding due to the elongated shear layer after separation, and thus has less lift fluctuations.

DISCUSSION

In this section, we discuss the mechanism of lift crisis. The fluctuations of lift and drag in flow over a circular cylinder is mainly caused by the roll-up of the Kármán vortices. Thus, the physical reason of lift crisis is understood with relation to the change in the Kármán vortex shedding at Re=1600.

Norberg (2003) paid attention to the fact that, with increasing Re from Re $\simeq$ 260, there is an increasing disorder in the fine-scale three dimensionalities associated with the secondary and essentially streamwise-oriented vortices of mode-B type (Williamson, 1996). He suggested that the augmentation of this mode-B type secondary vortices together with other small-scale motions and loosened spanwise coherency in the vortex shedding is responsible for the weakening of the Kármán vortex and causes the lift crisis. However, this conjecture is not so consistent to what we observe in this study. In general, the Strouhal number tends to decrease when the Kármán vortex rollers undergo three dimensional deformation. For example, when the mode-A type three-dimensional instability occurs and the Kármán vortex rollers suffer spanwise undulation, the Strouhal number drops (Williamson, 1996). A similar observation was also made in the case of active control. Kim and Choi (2005) applied a spanwisely varying distributed forcing to flow over a circular cylinder and observed that the Strouhal number is decreased when the Kármán vortex rollers are deformed three dimensionally. However, as shown in figure 4, the Strouhal number becomes maximum at lift crisis, implying that the lift crisis is not necessarily associated with the increased three-dimensionality and weakening of Kármán

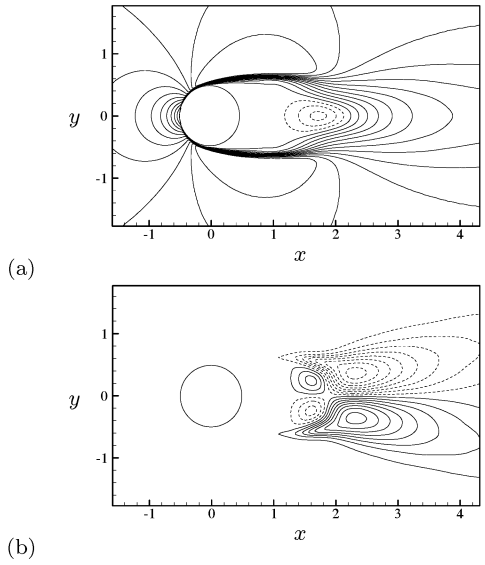

Figure 7: Time-averaged streamwise velocity and Reynolds shear stress: (a) $\bar{u}$; (b) $-\overline{u'v'}$.

vortex rollers.

On the other hand, we pay a special attention to the elongation of eddy formation region. We already showed that the thin shear layer persists down to $x \simeq d$ and there is almost no turbulence at $x < d$ in figures 2 and 7. Now, the spatial distributions of the time-averaged spanwise vorticity and mean-square pressure fluctuations are shown in figure 8. The elongation of thin separated shear layer can be seen in figure 8a. One can also recognize that the roll-up of Kármán vortices takes place at $x \simeq 2d$. The pressure fluctuations are concentrated at this vortex formation region and the fluctuations of pressure near the cylinder surface are very small (figure 8b). Accordingly, the lift fluctuation becomes small. Figure 9 shows the time-averaged spanwise vorticity and mean-square pressure fluctuations at Re=3900 (the levels of contours are the same as in figure 8). The separated shear layer is significantly shorter than that at Re=1600 and roll-up into the Kármán vortices occurs at $x \simeq 1.2d$. Since the roll-up position moves close to the cylinder, the cylinder is more exposed to the alternating motion of vortex shedding and the level of pressure fluctuations on the surface becomes high (figure 9b). From this observation, it is clear that the change in the eddy formation region is of great importance to understand the lift crisis.

CONCLUSION

In the present study, a large eddy simulation (LES) of flow over a circular cylinder was performed to investigate minimum lift fluctuations at Re=1600. The Strouhal number, lift fluctuations and pressure fluctuations on the cylinder surface showed excellent agreements with those from previous studies. It was shown that the flow over a circular cylinder at this Reynolds number is featured by elongated separated shear layer and delayed eddy formation. Therefore, the local minimum of lift fluctuation occurred around the present Reynolds number due to this long distance between the cylinder and the Kármán vortex roll-up position at which the fluctuating energy was concentrated.

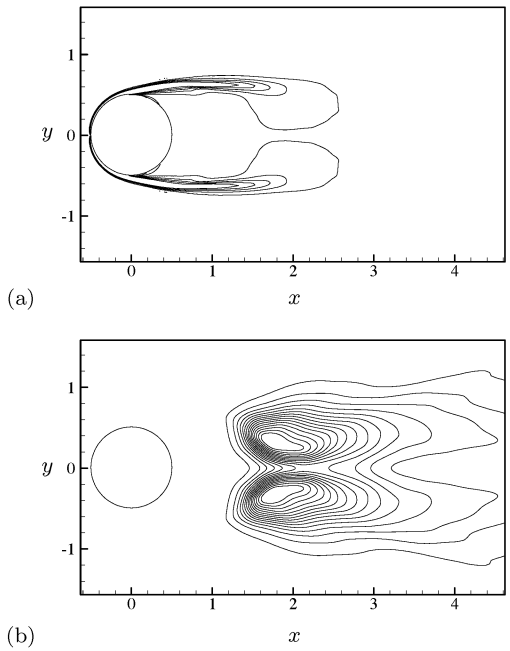

Figure 8: Contours of time-averaged spanwise vorticity and mean-square pressure fluctuations (Re=1600): (a) $\bar{\omega}_z$; (b) $\overline{p'^2}$.

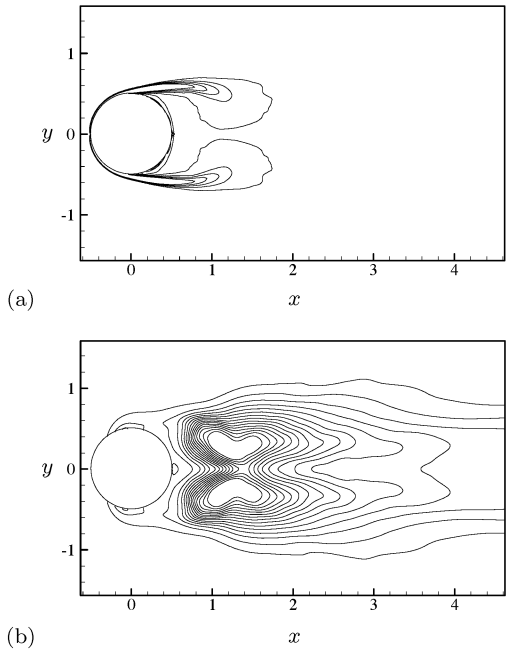

Figure 9: Contours of time-averaged spanwise vorticity and mean-square pressure fluctuations (Re=3900): (a) $\bar{\omega}_z$; (b) $\overline{p'^2}$.

REFERENCES

Choi, H., Moin, P. and Kim, J. 1993, "Direct numerical simulation of turbulent flow over riblets", *Journal of Fluid Mechanics*, Vol. 255, p. 503.

Germano, M., Piomelli, U., Moin, P. and Cabot, W. H., 1991, "A dynamic subgrid-scale eddy viscosity model", *Physics of Fluids* A, Vol. 3, p. 1760.

Jeong, J. and Hussain, F., 1995, "On the identification of a vortex", *Journal of Fluid Mechanics*, Vol. 285, p. 69.

Kim, J. and Choi, H., 2005, "Distributed forcing of flow over a circular cylinder", *Physics of Fluids*, Vol. 17, 033103

Lilly, D. K., 1992, "A proposed modification of the Germano subgrid scale closure method", *Physics of Fluids* A, Vol. 4, p. 633.

Norberg, C., 1998, "LDV-measurements in the near wake of a circular cylinder", *Proc. Advances in Understanding of Bluff Body Wakes and Vortex-Induced Vibration, Washington DC, June 1998*.

Norberg, C., 2003, "Fluctuating lift on a circular cylinder: review and new measurements", *Journal of Fluids and Structures*, Vol. 17, p. 57.

Williamson, C. H. K., 1996, "Three-dimensional wake transition", *Journal of Fluid Mechanics*, Vol. 328, P. 345.

Zdravkovich, M. M., 1997, Flow around circular cylinders, Oxford University Press.